

# Online Prediction of Driver Distraction Based on Brain Activity Patterns

Shouyi Wang, Yiqi Zhang, Changxu Wu, *Member, IEEE*, Felix Darvas, and  
Wanpracha Art Chaovaitwongse, *Senior Member, IEEE*

**Abstract**—This paper presents a new computational framework for early detection of driver distractions (map viewing) using brain activity measured by electroencephalographic (EEG) signals. Compared with most studies in the literature, which are mainly focused on the classification of distracted and nondistracted periods, this study proposes a new framework to prospectively predict the start and end of a distraction period, defined by map viewing. The proposed prediction algorithm was tested on a data set of continuous EEG signals recorded from 24 subjects. During the EEG recordings, the subjects were asked to drive from an initial position to a destination using a city map in a simulated driving environment. The overall accuracy values for the prediction of the start and the end of map viewing were 81% and 70%, respectively. The experimental results demonstrated that the proposed algorithm can predict the start and end of map viewing with relatively high accuracy and can be generalized to individual subjects. The outcome of this study has a high potential to improve the design of future intelligent navigation systems. Prediction of the start of map viewing can be used to provide route information based on a driver's needs and consequently avoid map-viewing activities. Prediction of the end of map viewing can be used to provide warnings for potential long map-viewing durations. Further development of the proposed framework and its applications in driver-distraction predictions are also discussed.

**Index Terms**—Driver-distraction prediction, electroencephalographic (EEG) signals, online adaptive predictions, time-series pattern recognition.

## I. INTRODUCTION

**D**ISTRACTED driving is one of the main causes of vehicle crashes. According to the statistics released by National Highway Traffic Safety Administration (NHTSA), 3092 people were killed, and 416 000 people were injured, in vehicle crashes involving distracted drivers in 2010 [1]. Driver distraction is defined as a form of inattention that “delayed the recognition of information needed to accomplish the driving task safely

because some event, activity, object, or person within or outside the vehicle compels or induces the driver's shifting attention away from the driving task” [2]. In particular, with the wide application of electronic route navigation systems, the navigation-map-viewing behavior becomes an important source of driving distraction and vehicle accidents. The serious safety issue has directed many researchers' attention to distracted driving performance that is associated with map-viewing behaviors and navigation systems. The corresponding human factors research of such systems is believed to contribute to the development of safe, usable, and acceptable assist systems to vehicle customers.

Navigation map viewing is a complex task, requiring the concurrent execution of various visual, motor, and cognitive skills, in addition to the driving task. Although map-viewing behavior is only a secondary task in driving, this activity is closely linked to the primary task of driving. A high number of studies have demonstrated that looking away from the road could result in driving performance decrement and raise significant safety issues [3]–[5]. Even when drivers have their eyes on the road, the cognitive distraction associated with in-vehicle devices can also have negative effects on driving performance [6]–[10]. This is because drivers may utilize too much cognitive capacity to process frequently received navigation information and, thus, pay less attention to the driving task and road conditions. Therefore, both visual distraction (e.g., map viewing) and cognitive distraction could lower driving performance and lead to dangerous situations [11], [12]. Moreover, another significant problem of using the current navigation systems is that frequent redundant information may be provided in some periods. The navigation information provided for route assistance may cause driving annoyance instead [13], [14]. A driver would feel annoyed since processing such redundant information takes significant resources from the already limited cognition capacity for the primary driving task.

To reduce the risk of driving distractions and avoid dangerous situations, eye movement tracking, video camera recognition, and lane keeping performance are popular techniques employed in current driver distraction studies [28], [35]. These methods have been proved to be effective in classifying distraction and nondistracted periods. However, they have limitations in detecting navigation-related distractions in real time. In recent years, many researchers have begun to use electroencephalographic (EEG) signals to study secondary tasks during driving [15]–[17]. EEG-based driving distraction studies offer a unique capability of real-time assessment of cognitive effort, engagement, and workload through quantitative analysis of continuous EEG signals. In addition, EEG signals are generally unaffected

Manuscript received September 26, 2013; revised February 5, 2014, February 12, 2014, and May 22, 2014; accepted May 29, 2014. The Associate Editor for this paper was S. Sun.

S. Wang was with the Department of Industrial and Systems Engineering, University of Washington, Seattle, WA 98195 USA. He is now with University of Texas at Arlington, Arlington, TX 76019 USA.

Y. Zhang and C. Wu are with the Department of Industrial and Systems Engineering, The State University of New York (SUNY), Buffalo, NY 14260 USA (e-mail: seanwu@buffalo.edu; changxu.wu@gmail.com).

F. Darvas is with the Department of Neurological Surgery, University of Washington, Seattle, WA 98105 USA (e-mail: fdarvas@u.washington.edu).

W. A. Chaovaitwongse is with the Department of Industrial and Systems Engineering, University of Washington, Seattle, WA 98195 USA (e-mail: artchao@uw.edu).

Color versions of one or more of the figures in this paper are available online at <http://ieeexplore.ieee.org>.

Digital Object Identifier 10.1109/TITS.2014.2330979

TABLE I  
SURVEY OF DRIVING DISTRACTION DATA COLLECTION METHODS

Data collection method	Studies	The period studied (Classification/Prediction)
Eye movement tracking	Chisholm, Caird, & Lockhart, 2008; Donmez, Boyle, & Lee, 2007, 2008, 2010; Garay-Vega et al., 2010; Kaber, Liang, Zhang, Rogers, & Gangakhedkar, 2012; Liang & Lee, 2010; Metz, Schömig, & Krüger, 2011; Reyes & Lee, 2008; K. L. Young, Mitsopoulos-Rubens, Rudin-Brown, & Lenné, 2012; H. Zhang, Smith, & Witt, 2006; Y. Zhang et al., 2013 [3], [4], [5], [7], [9], [18], [19], [24], [25], [26], [27], [28]	Classification of distracted and non-distracted period
Video camera recognition	Stutts et al., 2005; Wege, Will, & Victor, 2012 [29], [30]	Classification of distracted and non-distracted period
Lane-keeping Performance	Alm & Nilsson, 1995; Greenberg, Tijerina, & Curry, 2003; Reed & Green, 1999; Young, Lenné, & Williamson, 2011 [31], [32], [33], [34], [35]	Classification of distracted and non-distracted period
EEG	C. Lin, Ko, & Shen, 2009; C.-T. Lin, Chen, Chiu, Lin, & Ko, 2011; Mouloua, Ahern, & Quevedo, 2012; Sonnleitner, Simon, Kincses, Buchner, & Schrauf, 2012 [16], [36], [37], [38]	Classification of distracted and non-distracted period
	Current work	Prediction of the start (Event I) and the end (Event II) of distracted period

by driving conditions and environments. Studies showed that eye-movement-tracking techniques might become unstable in some driving environments [18]. For example, studies using eye trackers require an environment with dim illumination and low sunlight to minimize the glare and reflection [19]. An environment with strong glare and reflection could seriously deteriorate the performance of eye movement tracking [20]. Another advantage of EEG is its anonymous data in protecting the privacy for drivers. With the methods using eye movement tracking and video recognition it is difficult to avoid the privacy issue of leaking drivers' personal information, such as faces, expressions, or even conversations. In contrast, EEG signals only detect a driver's electronic brainwaves without recording any other personal information. In addition, with recent advances of EEG technologies, the conventional wet EEG electrodes requiring skin preparation and conduction gels may be replaced by wireless dry electrodes, which enable remote acquisition of continuous EEG data conveniently [21]–[23]. Thus, EEG technologies provide a practical approach to study driver behaviors and handle driving distractions in the real-world settings.

Table I summarizes the four main groups in current driving distraction studies. It is found that current studies are mostly focused on the retrospective classification of distracted periods and nondistracted periods. There have been very few studies focusing on real-time prospective prediction of driving distractions. With the help of EEG technologies, it may be possible to move from retrospective offline analyses to distinguish distraction and nondistracted periods to prospective online analyses to predict the initiation and the end of a distraction period. This study is aimed to address this transition and to provide a new framework for online detection of map-viewing distractions using continuous EEG signals. To be more specific,

two map-viewing actions (events) are studied: Event I is when the driver is starting to look at a map, and Event II is when the driver is starting to look back at the road. In the experiments, drivers were asked to arrive at a predefined destination in an unfamiliar environment using a city map. The task of navigating in an unfamiliar environment was employed in this study because it is cognitive demanding and well suited to study driver distractions [39].

The proposed framework was designed to predict the start and the end of map-viewing periods through online monitoring of EEG recordings. Once the prediction of Event I is achieved, future navigation systems can subsequently provide verbal route instructions in advance. Driver's view will then stay on the road, rather than looking at the map. As a result, the navigation system is able to prevent the incoming map-viewing actions, rather than letting drivers read the map themselves. Likewise, by predicting the time when the driver finishes a map-viewing behavior (Event II), the navigation system can provide a warning to the driver when the predicted map-viewing duration is longer than a safe threshold. The proposed real-time prediction framework has a high potential to improve the design of future route assist systems, including e-map and other intelligent navigation systems. The capabilities of providing route information based on a driver's needs and warnings to potential long map-viewing actions would greatly improve the efficiency of a navigation system with reduced annoyance and enhanced safety.

The rest of this paper is organized as follows: The driving experiment is discussed in Section II. In Section III, the online prediction framework is presented, including feature extraction, feature selection, adaptive prediction scheme, and the evaluation metrics of prediction performance. The computational experiments are provided in Section IV. A comprehensive



Fig. 1. Experiment setup using a STISIM driving simulator and a Neuroscan system including one Quik-Cap, Nuamps Express, and Scan software to record and analyze EEG signals during driving (the map for navigation is not included in this picture).

discussion of the impacts of this study is presented in Section V, and finally, we conclude this paper in Section VI.

## II. SIMULATED DRIVING EXPERIMENT

### A. Participants

Twenty-four participants (14 male and 10 female) took part in the current experiment with an average age of 23.3 ( $SD = 2.77$ ). All the participants have normal or corrected-to-normal vision and a valid driving license. They are also free of psychiatric or neurological disorders to limit potential confounds on the behavioral/cognitive aspects of driving performance and navigation activity.

### B. Apparatus

The driving task was completed using a STISIM driving simulator (STISIMDRIVE M100K, Systems Technology Inc., Hawthorne, CA; see Fig. 1). The driving simulator consists of a Logitech Momo steering wheel with force feedback, a gas pedal, and a brake pedal (Logitech Inc., Fremont, CA). The driving scenario was presented on a 27-in liquid-crystal display (LCD) with  $1920 \times 1200$  pixel resolution.

An  $8.5 \times 6$ -in map with designed route used for the map-viewing task was shown by a 19-in Dell LCD (1098FP model), which was 50 cm from the right hand of subjects and 91 cm from their eyes (see Fig. 3). The visual angle of the touch screen was  $13.1^\circ$ . The screen was controlled by a Dell PC (OPTIPLEX 745) and connected with the driving simulator via a Labjack system.

A Neuroscan system including one Quik-Cap, Nuamps Express, and Scan software was used to record and analyze EEG in the study. The Nuamps Express is a 40-channel digital EEG and event-related potential (ERP) recording system. There are four electrodes that were used for measuring eye movements to remove muscular artifacts. The rest 36 electrodes were mounted on the scalp and thus used for analyses in this paper. The

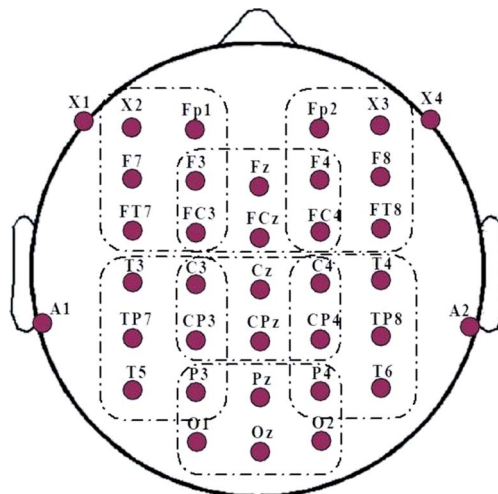


Fig. 2. Thirty-six EEG channels are divided into seven channel groups, according to their spatial locations. In the feature extraction stage, features are first extracted from each single channel and then averaged over each channel group.

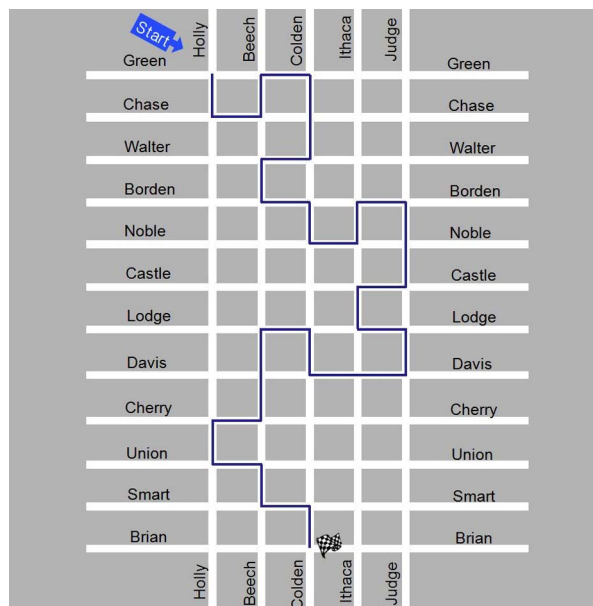


Fig. 3. Simulated city map employed in the driving experiment. Each subject was required to drive from an initial position to a destination indicated in the simulated city map.

placement of the 36 scalp electrodes is shown in Fig. 2. The SCAN software, i.e., a research-grade data processing tool, was employed to remove noise and artifacts or decompose complex signals. The EEG signals were amplified by the NuAmps Express system (Neuroscan Inc, USA) and sampled at 1000 Hz.

### C. Experimental Procedure

Participants seated themselves comfortably in the chair and wore a fitted EEG cap with 40 channels. After setting up the EEG cap, participants were trained for the driving and navigation task by completing a practice block. The practice block allowed participants to learn how to operate the driving simulator, including the steering wheel, speedometer, brake, and gas pedal. In addition, they could get familiar with the map-viewing

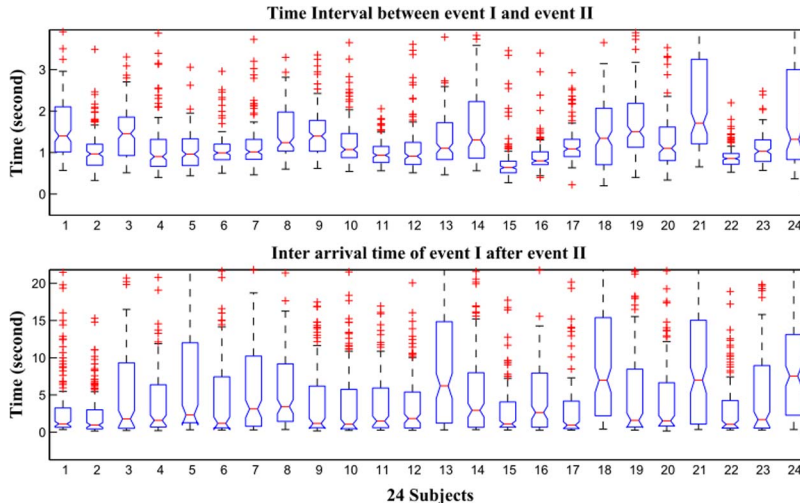


Fig. 4. Boxplots of the lengths of normal driving periods (interarrival intervals of Event I) and the lengths of the map-viewing periods. On each box, the central mark is the median, the edges of the box are the 25th and 75th percentiles, the whiskers extend to the most extreme data points that are not considered as outliers, and outliers are plotted individually by the red “plus” signs.

task along with the driving task. After the training segment, participants completed the test block by driving from an initial position to a destination indicated on the simulated city map, as shown in Fig. 3. The designed route was highlighted on the static map. In order to control potential confounding factors, drivers were constrained to look at the map for any route information. There was no verbal navigation instructions provided to distract drivers. In both practice and test blocks, participants were asked to operate the driving simulator by following normal traffic laws as if they were driving a vehicle in the real world. Continuous EEG signals were recorded during the driving tasks. The start and the end time of the map-viewing periods were also recorded.

#### D. Target Event Definition

Fig. 4 plots the statistics of the time lengths of the normal driving periods (interarrival periods of Event I) and the time lengths of map-viewing periods. The two target events to be predicted in this study were defined as follows:

- Normal Event I: Event I (starting to look at the map) after at least 5 s of continuous driving;
- Dangerous Event II: Event II (looking back to the road) after at least 2 s of map viewing.

We are particularly interested in the prediction of “normal Event I” because it is associated with the initiation of “uncertainty” of future route. The prediction of such event in driving is very insightful to provide navigation information timely based on a driver’s need. It is noted that a driver may look at the map back and forth a number of times in a short period. These short-time frequent glances can be considered in one route-learning process. The corresponding Event Is are considered less typical to represent the initiation of cognitive uncertainty for future driving route after a relatively long-term driving. Therefore, this study only focuses on the prediction of “*Normal Event Is*,” which are defined as the Event Is that have at least 5 s of driving prior to map viewing. The 5 s were chosen to eliminate the nonuncertainty-initiation-related Event Is [27], [40].

In addition, for Event II, we only focus on the “*dangerous Event II*” since we consider that the Event IIs with short map-viewing durations are much less dangerous than those with relatively longer off-road glance durations. The prediction of “dangerous Event IIs” is meaningful to provide warning in advance if the predicted time of looking back to the road exceeds a safety limit. According to [41], we employed 2 s as the criteria to identify the “dangerous Event IIs.”

### III. ATP PREDICTION FRAMEWORK

An adaptive-threshold-based (ATP) prediction framework was proposed to online monitor EEG signals and identify predictive patterns that are associated with Event I and Event II. The flowchart of the online prediction framework is shown in Fig. 5. In general, raw continuous EEG signals were monitored by a sliding window and converted to pattern clusters consecutively through a two-level feature extraction process. The probabilistic relationships between pattern clusters and the occurrences of Events I and II were estimated. If a pattern cluster is more likely to be in the pre-event (I or II) period, a corresponding event prediction is then triggered. Here, an overview of current EEG feature extraction techniques is discussed first, and then, the proposed two-level feature extraction, the pattern-cluster formulation, the probabilistic-rule-based prediction scheme, and the performance evaluation criterion are given in the following.

#### A. EEG Feature Extraction

Over the past decade, numerous studies have been performed to apply various quantitative methods to analyze EEG data. The statistical measures, such as mean and the higher order moments that include variance, kurtosis, and skewness, are commonly used features to study statistical properties of EEG signals at different mental states [48], [49]. Another group of popular feature extraction techniques investigate temporal morphological characteristics of EEG signal, such as curve length [50],

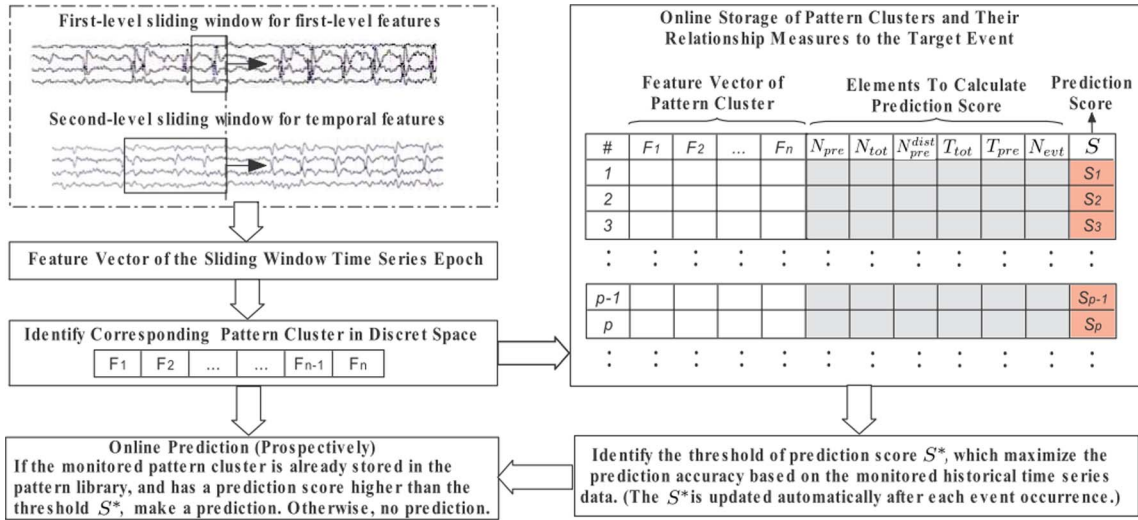


Fig. 5. Flowchart of the probabilistic ATP online prediction scheme using the concept of pattern cluster in discrete feature space.

zero crossings, number of peaks, and variance-to-range ratio [51], [52]. Energy is also an important feature for EEG signal classification. Some commonly used energy features include power spectrum analysis, nonlinear energy [53], extreme energy ratio [54], and extreme energy difference [55]. Since EEG data are multivariate signals, the interactions between EEG channels provide important information of brain dynamics. Various bivariate EEG features have also been used to study brain networks. Three commonly used bivariate features are Euclidean distance, correlation coefficient, and t-statistics [56]. The common spatial pattern (CSP) has been reported to be useful for detecting event-related desynchronization/synchronization (ERD/ERS). An adaptive CSP method has been developed recently to account for nonstationary properties of EEG signal [57]. In addition, various time–frequency analyses have also been developed for EEG feature extraction. The most well known time–frequency technique is wavelet transform (WT), which is capable of providing a representation of nonstationary EEG signals in both time and frequency domains accurately. In particular, wavelet entropy (WE) has become a popular feature to analyze EEG dynamics in recent years. WE is computed based on the relative energy associated with different frequency bands present in the EEG. It carries information about the degree of order/disorder of the wavelet energy distribution over the decomposed multifrequency EEG bands [58].

### B. First-Level Feature Extraction

As shown in Fig. 5, the first-level features are extracted directly from raw EEG signals through a sliding window. The employed feature extraction techniques covered the major feature categories discussed earlier, including univariate, bivariate, and time–frequency features as follows.

- *Univariate features*: Nine univariate features were extracted, including four statistical measures (*mean, variance, skewness, kurtosis*), three morphological features (*curve length, number of peaks, variance-to-range ratio*), and two energy related features (*signal power, average nonlinear energy*).

- *Bivariate features*: Three bivariate features were extracted pairwise within each channel group. The employed bivariate features include *pairwise Euclidean distance, pairwise T-statistics, and Pearson correlation coefficient*.
- *Time-frequency feature*: WE was employed to provide information about the degree of order/disorder associated with multifrequency EEG signal responses. It was calculated using discrete WT (DWT) for each channel of EEG. In addition, 36 EEG channels were divided into seven channel groups, according to their spatial locations (see Fig. 2 for exact locations). For univariate features and WE, they were first extracted from each EEG channel and then averaged within each channel group. For the bivariate features, they were first extracted for channel pairs within each channel group and subsequently averaged over all the pairs within each channel group. For an EEG epoch of 36 channels, there are  $7 \times 9 = 63$  univariate features +  $7 \times 3 = 21$  bivariate features +  $7 \times 1 = 7$  WE features = 91 features.

It should be noted that we applied sliding window with different sizes to monitor normal driving periods and map-viewing periods. This is because there were two events to predict. The prediction of Event I relied on the EEG signals in normal driving periods, whereas the prediction of Event II relied on the EEG signals in map-viewing periods. The two periods do not have any overlap. In a real-time monitoring process, the two independent prediction systems work interactively. If Event I is detected, the prediction system of Event II is turned on, and the prediction system of Event I is turned off, vice versa. As a result, two sliding windows were applied alternately to monitor raw EEG signals. In this paper, the length and step size of the Event I sliding window were 1 s and 100 ms, respectively, and the length and step size of the Event II sliding window were 250 ms and 25 ms, respectively.

### C. Second-Level Feature Extraction

The second-level feature extraction was designed to characterize temporal patterns of the first-level features. As shown in Fig. 5, a second-level sliding window was employed to monitor

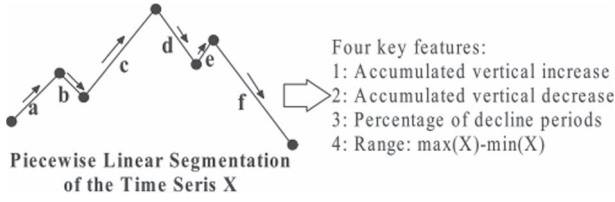


Fig. 6. Demonstration of the four second-level features obtained based on the piecewise linear segmentation of a first-level feature within the second-level sliding window. The four features were employed to represent the temporal fluctuation patterns of the first-level feature.

the time series of first-level features simultaneously with the first-level sliding window for raw EEG data. Different lengths of the second-level sliding window were tested from 1 to 5 s for Event I, and 500–1250 ms for Event II. Within a second-level sliding window, we first applied a piecewise linear approximation algorithm to partition the time series into piecewise linear segments. Then, we characterize temporal patterns of the time series by four features, as demonstrated in Fig. 6. For a time series  $X = (x_1, x_2, \dots, x_n)$ , its key-turning points are shown in the figure. There are six subsections, three of which (segment a, c, e) showing an uptrend, and three of which (segment b, d, f) showing a downtrend. These trends indicate the degree of fluctuation of the time series. The following four features are proposed to represent time-series fluctuation patterns:

Feature 1 is the accumulated vertical increase in the segmented piecewise linear time series, which is calculated as

$$F_{II1} = H(a) + H(c) + H(e) \quad (1)$$

where the function  $H(\cdot)$  means the vertical distance from the starting point to the ending point of a subsegment.

Feature 2 is the accumulated vertical decrease in the segmented piecewise linear time series, which is calculated as

$$F_{II2} = H(b) + H(d) + H(f). \quad (2)$$

Feature 3 is the percentage of the decreasing line segments, which is calculated as

$$F_{II3} = T(a + c + e)/T(X) \quad (3)$$

where  $T(\cdot)$  is the horizontal distance from the starting point to the ending point of a subsegment.

Feature 4 is the range of the time series, which is calculated as

$$F_{II4} = \max(X) - \min(X) \quad (4)$$

where  $\max(X)$  and  $\min(X)$  means the maximum and minimum values of the segmented time series, respectively.

#### D. Feature Selection

For each of the 91 first-level features, there are four second-level features associated with it. That is, there are  $91 \times 4 = 364$  feature candidates to represent each EEG epoch. However, not all of the extracted features are informative to the target events, and the high-dimensional feature space makes the online learning task extremely difficult to capture predictive pattern in a short period. Feature selection has to be performed

to achieve dimensionality reduction and find optimal feature subset. We employed Pudil's sequential floating search [42], which is popular to select the most discriminative features to separate data samples with two classes (in this study, pre-event and nonevent). There are two floating search schemes, which are called forward floating search (FFS) and backward floating search (BFS). Since FFS generally works faster than BFS when the expected number of selected features is much smaller than the complete feature dimension, we employed FFS in this study. Starting from an empty feature set, the FFS is basically a bottom-up search procedure, which includes new features and excludes the worst features in the current feature set sequentially to improve a class separability criterion. In this paper, the 1-nearest neighbor classification error was used as the separability measure. The objective of FFS is to select an optimal subset of features that minimize the 1-nearest neighbor classification error.

Let  $S_k$  be the feature subset of  $k$  features that have been selected from the complete feature set  $F_d = \{f_1, f_2, \dots, f_d\}$  using a criterion function  $E(X_k)$ . The values of  $E(X_i)$ , for all preceding subsets of size  $i = 1, 2, \dots, k - 1$ , are known and stored. The FFS procedure can be summarized as follows:

- Step 1 (Inclusion): Select the most significant feature  $f_i$  from the available feature set  $F_d - S_k$  to form the new feature set  $S_{k+1}$  by  $E(S_k + f_i) \leq E(S_k + f_j) < E(S_k)$ , where  $f_i, f_j \in F_d - S_k$  and  $i \neq j$ .
- Step 2 (Exclusion): Find the least significant feature  $f_p$  in the subset  $S_{k+1}$ , such that  $E(S_{k+1} - f_p) \leq E(S_{k+1} - f_q)$  for all  $f_q \in S_{k+1}$  and  $p \neq q$ . If  $E(S_{k+1} - f_p) < E(S_{k+1})$ , then exclude  $f_p$  from  $S_{k+1}$  to form a new feature set  $S'_k$ . We have  $E(S'_k) < E(S_{k+1})$ .
- Step 3 (Exclusion Continuation): Similar to step 2, continue to find the least significant feature  $f_m$  in the set  $S'_k$ . If  $E(S'_k - f_m) \geq E(S'_k)$ , then set  $S_k = S'_k$ ,  $E(S'_k) = E(S_k)$ , and return to step 1 for a new cycle of feature inclusion. If  $E(S'_k - f_m) < E(S'_k)$ , exclude  $f_m$  from  $S'_k$  to form a further reduced set  $S'_{k-1}$ . Set  $k = k - 1$ . Repeat step 3 if  $k > 2$ . If  $k = 2$ , set  $S_k = S'_k$ ,  $E(S'_k) = E(S_k)$ , and go to step 1.
- The FFS procedure stops when no features meet the criterion to be included in or to be removed from the current feature subset.

The floating search approaches take use of backtracking and are capable of correcting wrong inclusion/removal decisions. Floating search has become widely popular because it can often provide either the optimal or a close-to-optimal solution and also require much less computational time than the traditional branch-and-bound method and most other currently used suboptimal strategies. However, in the experiments with 364 features, FFS still took long computing time due to the huge amount of possible feature combinations to be tested. In addition, based on the testing prediction accuracy, we found that the obtained feature subset was suboptimal when compared with the features selected from a smaller pool of feature set.

To tackle the problem of "curse of dimensionality," we reduced the size of the feature candidates. In particular, we narrowed down the univariate features from nine to two, i.e.,

TABLE II  
FFS-SELECTED FEATURES FOR EVENT I

	Selected Feature	$f_1$	$f_2$	$f_3$	$f_4$	$f_5$	$f_6$	$f_7$	$f_8$	$f_9$	$f_{10}$
8-13 Hz	Channel Group	1	1	4	5	6	4	1	5	2	4
	First Level	$F_{I1}$	$F_{I2}$	$F_{I2}$	$F_{I1}$	$F_{I2}$	$F_{I1}$	$F_{I2}$	$F_{I2}$	$F_{I2}$	$F_{I2}$
	Second Level	$F_{II4}$	$F_{II1}$	$F_{II2}$	$F_{II4}$	$F_{II4}$	$F_{II4}$	$F_{II2}$	$F_{II4}$	$F_{II1}$	$F_{II1}$
13-30 Hz	Channel Group	6	1	1	3	4	3	4	2	4	2
	First Level	$F_{I1}$	$F_{I2}$	$F_{I2}$	$F_{I1}$	$F_{I2}$	$F_{I2}$	$F_{I1}$	$F_{I1}$	$F_{I1}$	$F_{I2}$
	Second Level	$F_{II4}$	$F_{II1}$	$F_{II2}$	$F_{II4}$	$F_{II2}$	$F_{II2}$	$F_{II4}$	$F_{II4}$	$F_{II2}$	$F_{II2}$
2-50 Hz	Channel Group	7	4	2	6	6	7	1	2	-	-
	First Level	$F_{I4}$	$F_{I4}$	$F_{I4}$	$F_{I3}$	$F_{I3}$	$F_{I3}$	$F_{I4}$	$F_{I1}$	-	-
	Second Level	$F_{II4}$	$F_{II4}$	$F_{II4}$	$F_{II1}$	$F_{II3}$	$F_{II1}$	$F_{II4}$	$F_{II4}$	-	-
1-100 Hz	Channel Group	5	7	7	1	4	2	3	2	5	-
	First Level	$F_{I4}$	$F_{I3}$	$F_{I4}$	$F_{I3}$	$F_{I3}$	$F_{I1}$	$F_{I1}$	$F_{I1}$	$F_{I1}$	-
	Second Level	$F_{II4}$	$F_{II2}$	$F_{II4}$	$F_{II2}$	$F_{II2}$	$F_{II2}$	$F_{II4}$	$F_{II4}$	$F_{II4}$	-

TABLE III  
FFS-SELECTED FEATURES FOR EVENT II

	Selected Feature	$f_1$	$f_2$	$f_3$	$f_4$	$f_5$	$f_6$	$f_7$	$f_8$	$f_9$	$f_{10}$
8-13 Hz	Channel	1	1	6	4	2	3	-	-	-	-
	First Level	$F_{I2}$	$F_{I2}$	$F_{I2}$	$F_{I2}$	$F_{I2}$	$F_{I2}$	-	-	-	-
	Second Level	$F_{II2}$	$F_{II1}$	$F_{II1}$	$F_{II1}$	$F_{II2}$	$F_{II2}$	-	-	-	-
13-30 Hz	Channel	6	2	3	1	5	4	2	5	7	2
	First Level	$F_{I1}$	$F_{I2}$	$F_{I2}$	$F_{I2}$	$F_{I2}$	$F_{I2}$	$F_{I2}$	$F_{I2}$	$F_{I2}$	$F_{I2}$
	Second Level	$F_{II4}$	$F_{II2}$	$F_{II4}$	$F_{II2}$	$F_{II1}$	$F_{II2}$	$F_{II4}$	$F_{II4}$	$F_{II4}$	$F_{II1}$
2-50 Hz	Channel	6	1	4	6	4	7	5	7	-	-
	First Level	$F_{I4}$	$F_{I3}$	$F_{I3}$	$F_{I3}$	$F_{I4}$	$F_{I3}$	$F_{I1}$	$F_{I4}$	-	-
	Second Level	$F_{II4}$	$F_{II2}$	$F_{II4}$	$F_{II3}$	$F_{II3}$	$F_{II4}$	$F_{II1}$	$F_{II3}$	-	-
1-100 Hz	Channel	5	5	1	4	6	2	2	4	7	2
	First Level	$F_{I4}$	$F_{I3}$	$F_{I3}$	$F_{I3}$	$F_{I3}$	$F_{I4}$	$F_{I1}$	$F_{I3}$	$F_{I3}$	$F_{I4}$
	Second Level	$F_{II4}$	$F_{II2}$	$F_{II1}$	$F_{II2}$	$F_{II2}$	$F_{II3}$	$F_{II1}$	$F_{II4}$	$F_{II1}$	$F_{II4}$

mean and curve length, and reduced the bivariate features from three to one, i.e., pairwise Euclidean distance. The other two bivariate features were excluded mainly because of their expensive cost of computing and, thus, may not fit well to a fast online prediction task. Together with the WE, we narrowed the first-level features to four candidates.

In addition, EEG signals are often described in terms of rhythmic activity and divided into frequency bands by using bandpass filters. To improve signal-to-noise ratio and also investigate EEG patterns in different brainwave bands, we analyzed EEG signals in four frequency bands: 8–13 Hz, 13–30 Hz, 2–50 Hz, and 1–100 Hz. The two frequency bands of 8–13 Hz and 13–30 Hz correspond to the well-known alpha and beta bands of brainwaves, respectively. Alpha is considered to be an important brain frequency to learn and use information. When alpha is within normal ranges, one tends to experience good moods and have a sense of conscious and calmness. Beta waves represent some “fast” cognitive activity of alert or anxious. The frequency band of 2–50 Hz contains the five most useful brain frequencies that EEG researchers tend to follow: delta (below 4 Hz), theta (4–7 Hz), alpha (8–13 Hz), beta (13–30 Hz), and low gamma (30–45 Hz). Finally, the EEG in the frequency band of 1–100 Hz can be considered the cleaned raw EEG data, for which the low frequency (< 1 Hz) and high frequency (> 100 Hz) noises are removed.

We performed FFS on the EEG of the four frequency bands separately and made online predictions for each frequency band separately. It is noted that the WE was calculated based on the energy of different frequency bands and indicates the order/disorder of energy distribution among different bands. Thus, it is meaningless for single-band signals in 8–13 Hz and 13–30 Hz. For the two single-band EEG signals, the first-level feature candidates were three: mean, curve length, and pairwise Euclidean distance. For EEG in 2–50 Hz and 1–100 Hz,

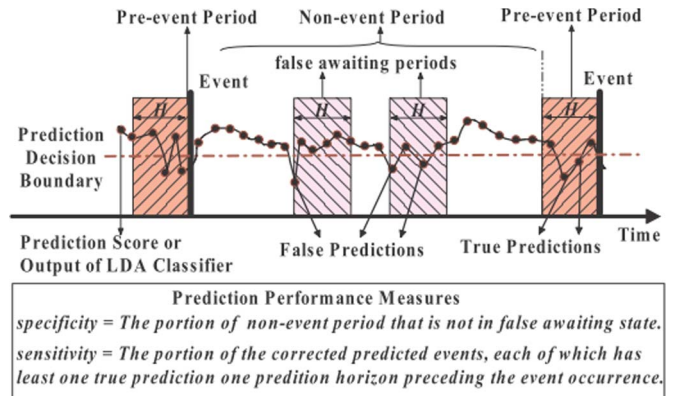


Fig. 7. Demonstration of the time-block-based sensitivity  $sen_{blk}$  and the time-block-based specificity  $spe_{blk}$ . The proposed  $sen_{blk}$  and  $spe_{blk}$  consider the effects of prediction horizon and, thus, are well suited to evaluate the online event-prediction problem.

we also found that the feature selection using three first-level features generated better prediction results than those using all the four candidates. The combination mean, pairwise Euclidean distance, and WE generated the best testing prediction performance. Thus, the experimental results of 2–50 Hz and 1–100 Hz reported in this paper were based on the selected features from a reduced feature set with these three first-level features. That is, the FFS was performed on a reduced feature set with 84 features (7 channel groups  $\times$  3 first-level features  $\times$  4 second-level features).

Let the four first-level feature candidates be denoted by:  $F_{I1}$  the averaged EEG signal within a channel group,  $F_{I2}$  the averaged curve length within a channel group,  $F_{I3}$  the averaged pairwise Euclidean distance within a channel group, and  $F_{I4}$  the averaged WE within a channel group. The FFS-selected features for events I and II are summarized in Tables II and III, respectively.

TABLE IV  
COMPUTATIONAL AND PARAMETER SETTINGS OF THE ADAPTIVE ONLINE PREDICTION FRAMEWORK

Parameter Setting	Setting Choices
Prediction Horizon	Event I: 400, 600, 800, 1000 ms Event II: 300, 400, 500 ms
1st-level sliding window (monitor raw time series)	Event I: window size 1000 ms, moving step 100 ms Event II: window size 250 ms, moving step 25 ms
2nd-level sliding window (monitor feature time series)	Event I: window size 1000, 2000, 3000, 4000, 5000 ms, moving step 100, 200, 300 ms Event II: window size 500, 750, 1000, 1250 ms, moving step 25 ms
Online Prediction Scheme	Adaptive Threshold-Based Prediction Scheme
Feature Selection Method	Pudil's floating search based on 1-Nearest Neighbour leave-one-out classification performance.
1st-level features	Nine univariate features: mean, variance, skewness, kurtosis, signal power, curve length, number of peaks, average nonlinear energy, variance to range ratio.
	Three pairwise bivariate measures: Euclidean distance, T-statistics, Pearson correlation.
	One time-frequency measure: wavelet entropy (features are averaged over each channel group as shown in Figure 2.4)
2nd-level features (temporal pattern feature)	1. Accumulated vertical increase 2. Accumulated vertical decrease 3. Percentage of decline periods 4. Amplitude range

TABLE V  
TRAINING AND TESTING PREDICTION RESULTS FOR EVENT I AVERAGED OVER THE 24 SUBJECTS USING THE BEST PARAMETER OVER DIFFERENT PREDICTION HORIZONS AND FREQUENCY BANDS

Frequency Band (Hz)	Horizon (ms)	Training		Testing	
		$Sen_{blk}$	$Spe_{blk}$	$Sen_{blk}$	$Spe_{blk}$
8-13 Hz	400	0.71	0.77	0.77	0.63
	600	0.72	0.72	0.76	0.56
	800	0.85	0.57	0.81	0.51
	1000	0.81	0.55	0.81	0.51
13-30 Hz	400	0.67	0.75	0.71	0.68
	600	0.71	0.71	0.77	0.62
	800	0.73	0.68	0.83	0.55
	1000	0.73	0.66	0.82	0.55
2-50 Hz	400	0.82	0.90	<b>0.79</b>	<b>0.83</b>
	600	0.87	0.82	0.83	0.75
	800	0.88	0.8	0.83	0.71
	1000	0.88	0.78	0.85	0.67
1-100 Hz	400	0.34	0.89	0.39	0.8
	600	0.48	0.77	0.52	0.68
	800	0.56	0.72	0.63	0.61
	1000	0.6	0.67	0.69	0.55

As summarized in Tables II and III, the selected features form a feature vector to represent the “pattern” of each monitored EEG epoch in the sliding window.

### E. Pattern Cluster in a Discrete Feature Space

For the selected features, we partitioned each feature space into a number of nonoverlapping intervals using linear equi-volume partitioning. The continuous feature vectors were discretized into feature clusters, each of which represents a set of close-by patterns with similar underlying cognitive activities. In other words, we encode brain activities into a limited number of pattern clusters. We explored different numbers of partition bins ranging from 4 to 10. The partition with eight intervals obtained relative better results and thus reported in this study. For example, for an 8-D feature space with each dimension partitioned into eight intervals, the total number of all possible pattern clusters was  $8^8 = 16777216$ , which accounted for numerous brain activities during driving. Although this was a very large number, our experiments showed that recorded pattern clusters were in a level of 1000.

TABLE VI  
PREDICTION TIME STATISTICS OF EVENT I AVERAGED OVER THE 24 SUBJECTS USING THE BEST PARAMETER OVER DIFFERENT PREDICTION HORIZONS AND FREQUENCY BANDS

Frequency Band	Horizon (ms)	Statistics of Prediction Time for Event I			
		Training		Testing	
		mean (ms)	std.	mean (ms)	std.
8-13Hz	400	241.61	169.74	291.55	152.01
	600	385.98	249.94	475.08	201.89
	800	520.42	331.51	642.72	269.47
	1000	761.97	348.11	851.86	275.05
13-30Hz	400	81.29	147.60	81.27	149.59
	600	151.59	240.10	181.79	257.19
	800	208.50	319.52	274.66	345.14
	1000	304.95	414.72	410.37	445.55
2-50Hz	400	200.00	178.40	234.20	176.44
	600	336.65	266.40	381.65	244.33
	800	495.54	332.64	591.40	284.74
	1000	633.33	411.35	756.21	354.09
1-100Hz	400	244.81	171.24	297.91	152.13
	600	395.34	244.83	484.08	197.79
	800	553.26	317.99	651.32	266.50
	1000	737.25	358.06	847.44	277.44

### F. Probabilistic Prediction Score

A probabilistic prediction score was introduced to identify predictive pattern clusters to the two target events. The prediction score of a pattern cluster for predicting an event was associated with its likelihood in the pre-event period based on its occurrence frequency analysis. The probabilistic prediction score is defined as follows.

1) *Prediction Score*: Given a pattern cluster indexed as the  $k$ th cluster in the pattern-recording table, its prediction score  $S_k$  is defined as

$$S_k = \frac{N_{pre}/N_{tot}}{R_{pre}} \times \frac{N_{pre}^{dist}}{N_{evt}} \quad (5)$$

where  $N_{pre}$  is the number of occurrences of the pattern cluster in all previously monitored pre-event periods;  $N_{pre}^{dist}$  is the number of pre-event periods such that the pattern cluster appears at least once in each of them;  $N_{tot}$  is the total number of occurrences of the pattern cluster; and  $N_{evt}$  is the total number of events that have occurred. Finally,  $R_{pre}$  is the time ratio



TABLE VII  
TRAINING AND TESTING RESULTS OF EVENT I FOR 24 INDIVIDUAL SUBJECTS USING  
THE PREDICTION HORIZON OF 400 MS AND THE FREQUENCY BAND OF 2–50 HZ

Subject	Settings			Training		Testing	
	$L_{mw}$ (ms)	$L_{step}$ (ms)	Horizon (ms)	$sen_{blk}$	$spe_{blk}$	$sen_{blk}$	$spe_{blk}$
1	5000	100	400	0.77	0.95	0.75	0.88
2	4000	100	400	0.85	0.91	0.69	0.89
3	5000	100	400	0.86	0.88	0.86	0.75
4	5000	100	400	0.88	0.86	0.81	0.69
5	5000	100	400	0.71	0.91	0.79	0.89
6	3000	100	400	0.80	0.94	0.79	0.82
7	4000	100	400	0.79	0.93	0.72	0.83
8	5000	100	400	0.81	0.94	0.87	0.87
9	3000	100	400	0.75	0.97	0.80	0.94
10	3000	100	400	0.76	0.92	0.94	0.84
11	3000	100	400	0.93	0.85	0.85	0.73
12	3000	100	400	0.84	0.87	0.74	0.78
13	3000	100	400	0.87	0.88	0.86	0.81
14	4000	100	400	0.76	0.92	0.85	0.80
15	4000	100	400	0.75	0.90	0.82	0.85
16	3000	100	400	0.89	0.82	0.65	0.77
17	4000	100	400	0.88	0.96	0.71	0.95
18	4000	100	400	0.71	0.86	0.93	0.85
19	3000	100	400	0.79	0.91	0.56	0.90
20	4000	100	400	0.94	0.78	0.89	0.76
21	5000	200	400	0.82	0.74	0.50	0.87
22	4000	100	400	0.85	0.98	0.83	0.90
23	5000	100	400	0.79	0.87	0.77	0.73
24	4000	100	400	0.89	0.96	0.94	0.90
Ave.				0.82	0.90	0.79	0.83
PA				0.86		0.81	

between pre-event periods and nonevent periods. In particular, it is calculated as

$$R_{pre} = \frac{T_{pre}}{T_{tot} - T_{pre}} = \frac{N_{evt} \times T_{hrzn}}{T_{tot} - N_{evt} \times T_{hrzn}} \quad (6)$$

where  $T_{pre}$  is the total length of monitored pre-event periods,  $T_{tot}$  is the total length of the monitored EEG time series, and  $T_{hrzn}$  is the length of prediction horizon.

The predictive score proposed in (5) indicates how strong a pattern cluster is associated with the target event. In particular, the first term of (5) is to evaluate if the pattern cluster occurs in pre-event periods at a random level. If the pattern is purely random in both pre-event periods and nonevent periods, then we have  $E(N_{pre}/N_{tot}) = E(R_{pre})$ . If the pattern occurs more frequently in pre-event periods than the nonevent periods, we have  $E(N_{pre}/N_{tot}) > E(R_{pre})$ . The higher the ratio value, the more likely the pattern cluster is associated with the target event. If the pattern occurs less frequently in pre-event periods than the nonevent periods, we have  $E(N_{pre}/N_{tot}) < E(R_{pre})$ . The second term of (5) is to evaluate if a pattern cluster occurs in many pre-event periods. We expect that an ideal candidate of predictive pattern should appear in most pre-event periods, not only in a few ones. That is  $N_{pre}^{dist}/N_{evt} \approx 1$ . In summary, (5) estimates the likelihood of a pattern cluster in the pre-event period and reduces the bad effects of some extreme situations. In general, the higher the prediction score, the higher the probability that the pattern cluster appears in the pre-event period and, thus, the more prominent it is to predict events.

2) *Score-Based Prediction Rule*: The pattern-recording table stores and summarizes the recorded pattern clusters and calculates their prediction scores according to (5). We employed an adaptive threshold on the prediction score to discriminate the pre-event and nonevent pattern clusters. *Since for the recorded patterns we already know their class (event or pre-event) and*

*prediction scores, for any given score threshold, it is convenient to calculate the corresponding prediction accuracy (sensitivity and specificity) retrospectively. We employed a heuristic search approach to set the optimal value of the threshold  $S_*$  adaptively after each occurrence of the target event. In particular, we tried 30 values within the current recorded prediction score range ( $S_{max} - S_{min}$ ), starting from 1/30 of the range with an increment of 1/30 range each time. The optimal threshold  $S_*$  is set to the value that maximized the overall prediction performance (sensitivity + specificity) based on prediction scores of previously recorded patterns. The threshold  $S_*$  was updated after each occurrence of a target event. The prediction rule works as follows. For example, a sliding-window-monitored EEG epoch is converted to a pattern cluster, which is the  $k$ th cluster in the pattern-recording table. The corresponding prediction score is denoted by  $S_K$ . Then, the prediction rule is defined by:*

$$predictor = \begin{cases} 1, & \text{if } S_K > S_* \text{ (make a prediction)} \\ 0, & \text{otherwise (no prediction).} \end{cases}$$

### G. Evaluation of Prediction Performance

The most commonly used prediction performance measures are specificity and sensitivity. However, the traditional definition of specificity and sensitivity only focus on the correctness of each individual prediction and do not consider the prediction horizon and event-specific information. They are inappropriate to measure prediction performance directly for the online prediction problem, which has to consider the effects of prediction horizon and the event-specific requirements. Thus, we proposed a modified version of sensitivity and specificity that are well suited to evaluate the online event-prediction problem. In particular, we introduced a time-block-based sensitivity, denoted by  $sen_{blk}$ , which is defined as the portion of correctly predicted events in the total number of events. An event is

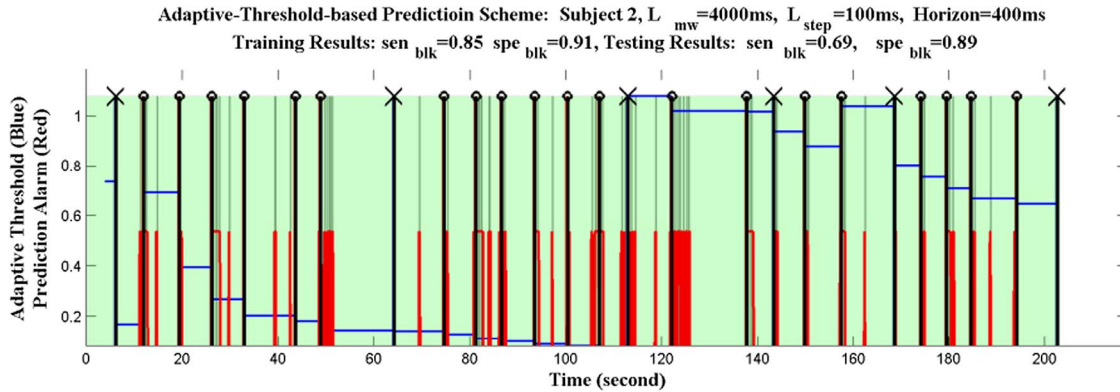


Fig. 8. Demonstration of the prediction outcome of Event I in Subject 2 using the prediction horizon of  $H = 400$  ms, with  $L_{mw} = 4000$  ms and  $L_{step} = 100$  ms in the frequency band of 2–50 Hz. The vertical black lines indicate the starting times of Event I. The cross sign on top of a vertical black line indicates that the system failed to predict the corresponding Event I within the prediction horizon of 400 ms. The circle sign on top of a vertical black line indicates that the corresponding Event I was successfully predicted. The vertical red lines represent the timing of the predictions. The horizontal blue lines represent the threshold level, whose value is updated after each occurrence of Event I.

considered to be correctly predicted if there is at least one true prediction within its preceding prediction horizon. According to Mormann *et al.* [43], we also employed a time-block-based specificity, denoted by  $spe_{blk}$ , which is defined as the portion of nonevent time period that is not in false awaiting state. A demonstration of the  $sen_{blk}$  and  $spe_{blk}$  quantification is shown in Fig. 7.

#### IV. COMPUTATIONAL EXPERIMENTS

##### A. Computational Settings

The proposed prediction framework was implemented and tested on the EEG recordings of 24 subjects for both “normal Event I” and “dangerous Event II.” The complete parameter settings of the prediction framework discussed in the previous section are summarized in Table IV.

##### B. Experimental Results

For the prediction of Event I, the averaged training and testing results over the 24 subjects for different prediction horizons and frequency bands are summarized in Table V. The best testing performance of our prediction algorithm was achieved with a  $sen_{blk}$  of 0.79 and a  $spe_{blk}$  of 0.83, using a prediction horizon of 400 ms in the frequency band of 2–50 Hz. The average and standard deviation of prediction times are provided in Table VI. The detailed prediction results of Event I for individual subjects based on the best prediction horizon and frequency band are shown in Table VII.

Fig. 8 illustrates an example of the prediction results of Event I in Subject 2 using the best training parameter settings. In the figure, it can be observed that our prediction algorithm yielded accurate prediction performance for the prediction of Event I. The high specificity achieved by our algorithm indicates that our framework is robust to signal noises because an alarm is only triggered when a monitored pattern cluster is already identified as a pre-event pattern with a higher than threshold prediction score in the pattern-recording table. All other noisy patterns cannot trigger any warning alarms.

For the prediction of Event II, the training and testing results averaged over the 24 subjects are reported in Table VIII. The

TABLE VIII  
TRAINING AND TESTING RESULTS OF EVENT II AVERAGED OVER THE 24 SUBJECTS WITH THE BEST PARAMETER OVER DIFFERENT PREDICTION HORIZONS AND FREQUENCY BANDS

Frequency Band	Horizon (ms)	Training		Testing	
		$sen_{blk}$	$spe_{blk}$	$sen_{blk}$	$spe_{blk}$
8-13 Hz	300	0.82	0.54	0.98	0.40
	400	0.80	0.51	0.99	0.37
	500	0.83	0.47	0.99	0.31
13-30 Hz	300	0.80	0.60	0.93	0.47
	400	0.82	0.57	0.96	0.44
	500	0.78	0.59	<b>0.96</b>	<b>0.45</b>
2-50 Hz	300	0.72	0.66	0.77	0.53
	400	0.76	0.63	0.82	0.49
	500	0.75	0.61	0.86	0.46
1-100 Hz	300	0.72	0.65	0.76	0.51
	400	0.74	0.63	0.80	0.49
	500	0.72	0.61	0.83	0.44

TABLE IX  
PREDICTION TIME STATISTICS OF EVENT II AVERAGED OVER THE 24 SUBJECTS USING THE BEST PARAMETER OVER DIFFERENT PREDICTION HORIZONS AND FREQUENCY BANDS

Frequency Band	Horizon (ms)	Statistics of Prediction Time for Event II			
		Training		Testing	
		mean	std.	mean	std.
8-13Hz	300	254.13	85.43	276.4	59.45
	400	338.28	106.56	370.57	75.57
	500	427.09	133.79	452.4	110.21
13-30Hz	300	213.83	108.95	240.6	88.47
	400	308.21	128.65	351.44	87.15
	500	382.48	156.6	429.78	117.51
2-50Hz	300	207.04	118.6	245.3	96.44
	400	297.98	141.5	330.07	123.9
	500	376.75	170.82	426.88	133.74
1-100Hz	300	261.71	84.84	278.93	58.86
	400	357.7	98.16	373.37	81.65
	500	443.72	120.96	478.78	71.67

best testing performance was achieved with a  $sen_{blk}$  of 0.96 and a  $spe_{blk}$  of 0.45, using the prediction horizon of 500 ms and the frequency band of 13–30 Hz. The average and standard deviation of prediction times are provided in Table IX. Detailed prediction results for individual subjects are shown in Table X. Note that the prediction performance of Event II was worse than that of Event I. We postulate that, in addition to the driving task, the map-viewing process requires concurrent execution of various cognitive, visual, and motor activities in a short period; EEG signals are more complex; and it is harder to discover predictive patterns that are associated with the intention of looking back to the road.

TABLE X  
TRAINING AND TESTING RESULTS OF EVENT II FOR 24 INDIVIDUAL SUBJECTS USING  
THE PREDICTION HORIZON OF 500 MS AND THE FREQUENCY BAND OF 13–30 HZ

Subject	Settings			Training		Testing	
	$L_{mw}$ (ms)	$L_{step}$ (ms)	Horizon (ms)	$sen_{blk}$	$spe_{blk}$	$sen_{blk}$	$spe_{blk}$
1	1250	25	500	0.60	0.64	0.87	0.41
2	750	25	500	0.97	0.27	1.00	0.28
3	1000	25	500	0.83	0.77	1.00	0.51
4	1000	25	500	0.75	0.57	1.00	0.29
5	750	25	500	0.50	0.65	1.00	0.49
6	1000	25	500	0.75	0.48	1.00	0.76
7	1000	25	500	0.60	0.59	1.00	0.42
8	1250	25	500	0.60	0.68	0.67	0.53
9	1250	25	500	0.86	0.64	1.00	0.62
10	1250	25	500	0.80	0.66	1.00	0.66
11	500	25	500	1.00	0.66	1.00	0.39
12	1250	25	500	0.67	0.69	0.60	0.54
13	1000	25	500	0.80	0.54	1.00	0.48
14	1250	25	500	0.86	0.50	1.00	0.30
15	500	25	500	0.96	0.29	1.00	0.12
16	1000	25	500	1.00	0.46	1.00	0.46
17	1250	25	500	0.67	0.82	1.00	0.80
18	1250	25	500	0.83	0.62	1.00	0.52
19	1000	25	500	0.87	0.40	0.93	0.28
20	1000	25	500	0.60	0.64	1.00	0.50
21	1250	25	500	0.85	0.31	1.00	0.38
22	750	25	500	0.80	0.81	1.00	0.15
23	750	25	500	0.88	0.84	1.00	0.62
24	1250	25	500	0.70	0.56	0.89	0.31
Ave.				0.78	0.59	0.96	0.45
PA				0.68		0.70	

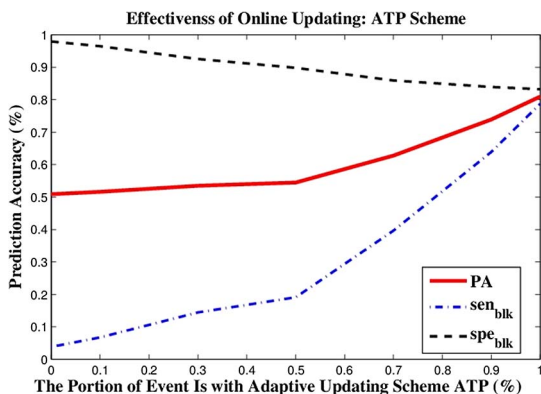


Fig. 9. Effectiveness of the adaptive threshold-updating scheme using the EEG data in the frequency band of 2–50 Hz. The horizontal axis indicates the portion of events in which the threshold of the ATP scheme was actively updated. The point 0 indicates that the initial score threshold was unchanged throughout the prediction process, and the point 1 means that the threshold was updated for all events throughout the entire prediction process. The strong increase trend of prediction accuracy indicates that the adaptive updating scheme ATP is effective to increase online prediction performance over time.

### C. Effectiveness of Adaptive Updating

The threshold level of the prediction score was updated (optimized) after each event. To test the effectiveness of the adaptive threshold-updating scheme, we compared the prediction performances for different updating periods in the frequency band of 2–50 Hz. In particular, for each subject, we updated the threshold in the first 0%, 10%, 30%, 50%, 70%, 90%, and 100% of the total target events, respectively. That is, 0% means that the initial threshold was unchanged throughout the prediction process, and 100% means that the threshold was updated for all events. Fig. 9 plots the averaged prediction performances of the seven different parameters of updating periods. It can be seen that the overall prediction accuracy values increased as the portion of EEG data used to update the threshold increased. The strong increase trend of prediction accuracy indicates that

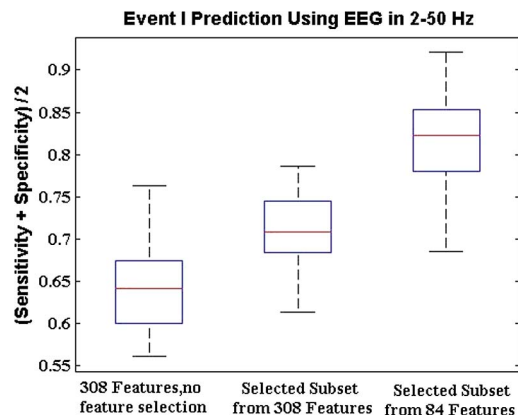


Fig. 10. Boxplot of the testing performance of Event I prediction for the 24 subjects in 2–50 Hz, using all 308 features, the selected features from the 308 features, and the selected features from a reduced set with 84 features, respectively. The feature set with 308 features was formed by 11 first-level features (9 univariate features + pairwise Euclidean distance + wavelet entropy)  $\times$  4 second-level features  $\times$  7 EEG channel groups. The feature set with 84 features used four first-level features (mean, curve length, pairwise Euclidean distance, and WE).

the adaptive threshold-updating scheme is truly effective in increasing the prediction performance over time.

### D. Effectiveness of Feature Selection

As discussed in Section III-C, we did experiments with different sizes of feature candidates. Figs. 10 and 11 show the prediction performance using three different feature sets. The first feature set is the complete feature set with all extracted features. The second feature set is the FFS-selected feature subset from the complete feature set. The third feature set is the FFS-selected feature subset from feature sets with reduced number of features. We discussed how we selected the reduced feature set in a heuristic manner, in Section III-C. The prediction performance boxplots clearly show that the complete feature

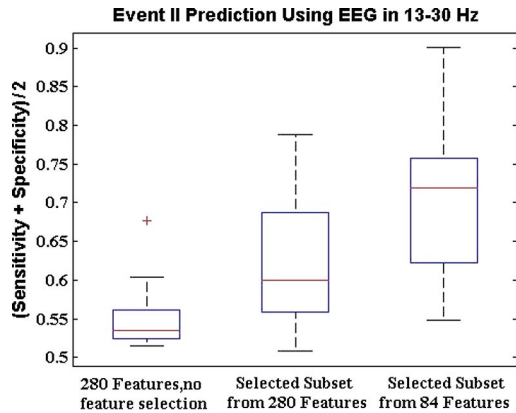


Fig. 11. Boxplot of the testing performance of Event II prediction for the 24 subjects in 13–30 Hz, using all 280 features, the selected features from the 280 features, and the selected features from a reduced set with 84 features, respectively. The feature set with 280 features was formed by 10 first-level features (9 univariate features + pairwise Euclidean distance)  $\times$  4 second-level features  $\times$  7 EEG channel groups. The feature set with 84 features used four first-level features (mean, curve length, and pairwise Euclidean distance).

set with around 300 features generated the worst prediction performance. The FFS-selected features from the complete feature set generally improved the prediction performance across the 24 subjects. However, it clearly provided a suboptimal solution since the FFS-selected features from a reduced feature set generated considerably better prediction results (the reduced feature set is a subset of the complete subset). Currently, the feature selection problem is still an open question for a high-dimensional data-mining task. Better feature selection frameworks are needed to search for the optimal feature subset in a high-dimensional space while maintaining a good performance/speed ratio.

## V. DISCUSSION

### A. Prediction Performance

There has been an explosion research on detection of driver state for driving assistance systems. However, very few investigations have been performed on real-time prospective prediction of cognitive activity. Most of the current studies were concentrated on the detection or predictability of mental states. Recently, Stefan *et al.* have investigated the online prediction of a driver’s intention to brake before any actions become observable [44]. A linear discriminant analysis classifier was trained using the EEG signals between the 260-ms preresponse and the response onset. The detection rate was 80%, using the combination of features of EEG, electromyography (EMG), and several driver behavior features. The false alarm rate was 1.96 per hour, and the average alarm time was 167 ms. Berka *et al.* employed EEG data to monitor the levels of task engagement and mental workload continuously in an operational environment [45]. A second-by-second classification was applied to detect workload in different engagement levels. A problem of the existing approaches is that the trained online classifier cannot be adaptive to each person and thus limit their prediction performance and application potentials. In this paper, we develop an adaptive prediction framework to predict driver distraction prospectively. The proposed ATP scheme generated very promising prediction

results based on a data set of 24 subjects. Using the best training parameter settings, the average testing sensitivity and specificity of the ATP scheme are 79% and 83%, respectively, to predict the intention of looking to the map.

The probabilistic ATP scheme constructs a pattern library for each subject specifically and gains the predictive pattern knowledge of each subject over time. With the pattern-cluster approach in discrete feature space, the size of the pattern library is limited. In real-life applications, the pattern-cluster library only takes a very small space and is extremely computational efficient. In this experiment, the total number of stored pattern clusters for each subject is at a level of 1000, and the number of identified pre-event pattern clusters is at a level of 100. Another significant advantage of the ATP scheme is that it is not sensitive to pattern noises and outliers in the online monitoring process. A prediction is only triggered if the monitored pattern cluster is already identified as a pre-event pattern cluster in the pattern library. All other monitored patterns (including any pattern noises and outliers) cannot trigger any warning alarms. This makes the proposed probabilistic ATP prediction very attractive in real-life applications. The proposed ATP prediction framework provides a useful analytical tool for online monitoring and prediction of driver distraction using multichannel EEG signals.

### B. Application of Prediction of Two Events in Developing Information Systems

Previous work laid the foundation to differentiate distracted periods from nondistracted periods during driving. When drivers look at a map for route information, distraction is inevitable to some extent. Therefore, the proposed prediction approach of driving distraction has a potential to prevent the driver distraction in advance or at least help to reduce the extent of distraction and its resulting hazards. With such approach being applied, in-vehicle navigation systems can be improved by adopting a need-based design.

1) *Application of Prediction of “Normal Event I”*: The prediction of “normal Event I” can be applied to prevent head-turning distraction in advance. An improved design of navigation systems can be achieved by integrating the capability of predicting drivers’ needs of route information. In other words, the route information would be presented only when a driver is uncertain about route and intends to look at the map for assistance. The route information provided in advance would prevent drivers from being distracted by reading a map passively; meanwhile, the redundant/unnecessary navigation information, which leads to drivers’ annoyance and takes up cognitive resources from the primary driving task, would be reduced.

The rules presented in Table XI with respect to “Normal Event I” can be applied in the design of navigation and warning systems.  $T_{p1}$  is the prediction time ahead of the occurrence of Event I, and  $T_r$  is the average simple braking reaction time of auditory stimuli, which is 514 ms [46], [47].

When  $T_{p1}$  is longer than  $T_r$ , route information can be delivered before the driver looks at the map. If there is no hazard detected (or unknown), then the driver will obtain the route information without being distracted from the road. Thus, the risk

TABLE XI  
APPLICATION OF PREDICTION OF “NORMAL EVENT I”  
IN NAVIGATION SYSTEM DESIGN

Hazard detection	Condition	System Operation
No/ Unknown	$T_{p1} > T_r$	Provide verbal route information in advance to avoid the map-viewing activity
	$T_{p1} < T_r$	Switch on the prediction of ‘dangerous Event II’
Yes	$T_{p1} > T_r$	Provide a verbal warning: Do not look away from the road
	$T_{p1} < T_r$	Provide a verbal warning: Look back to the road immediately.

of eye-off-road can be largely reduced. However, when  $T_{p1}$  is shorter than  $T_r$ , the map-viewing action cannot be avoided since the driver may already start looking at the map when the route information is presented. Thus, the system lets the driver keep on reading maps rather than interrupting the driver by providing the route information to add on additional distraction. At this time, the prediction of “dangerous Event II” is switched on, and the system will provide warnings to the driver in advance if the predicted map-view duration is longer than the safety threshold.

When there is a hazard event being detected and  $T_{p1}$  is longer than  $T_r$ , the system would alarm the driver to watch out for the hazard and do not look away from the road. However, when  $T_{p1}$  is shorter than  $T_r$ , the driver may already look at the map when the warning message is provided. Therefore, the message should warn the driver to look back to the road and pay attention to the detected hazard.

2) *Application of Prediction of “Dangerous Event II”*: The prediction of “dangerous Event II” can be used to design a warning system to reduce the risk of long-time map-viewing activities in driving. When looking at a map, a driver loses attention to the driving task and road conditions. Thus, the map-viewing behavior would result in an impaired driving performance and may lead to dangerous situations. With the capability of predicting “dangerous Event II,” the system can predict the time duration of a map-viewing process ahead of time. If the predicted time duration of the map-viewing process exceeds a safe time length, the system can warn the driver ahead of time to look back and turn attention to road conditions.

The rules presented in Table XII with respect to “dangerous Event II” can be applied to design navigation and warning systems. The prediction of Event II is triggered after Event I initiated and will be repeated by the system after a certain time interval, which is equal to the length of prediction horizon ( $T_{hrzn}$ ).  $N$  denotes the number of time intervals before the system predicts that Event II will start.  $T_{p2}$  is the prediction time ahead of the occurrence of Event II after the  $N$ th prediction. The summation of  $N \times T_{hrzn}$  and  $T_{p2}$  denotes the predicted time duration of map-viewing task from the Event I being initiated to the predicted occurrence of Event II. If the time interval ( $N \times T_{hrzn} + T_{p2}$ ) is larger than the safety threshold, a warning is to be generated. The safety threshold is set to 2 s to select long map-viewing periods with high risk during driving [43].

A longer  $T_{p2} + N \times T_{hrzn}$  than the safety threshold indicates that the duration of eye-off-road may exceed the safety limit. Therefore, when there is no hazard detected (or no hazard-

TABLE XII  
APPLICATION OF PREDICTION OF “DANGEROUS EVENT II”  
IN NAVIGATION SYSTEM DESIGN

Hazard detection	Condition	System Operation
No/ Unknown	$N \times T_{hrzn} + T_{p2} > \text{safety threshold}$	Provide a warning in advance to prevent longer duration of maps-viewing and decrease the associated driving risks
	$N \times T_{hrzn} + T_{p2} < \text{safety threshold}$	Keeps on predicting the ‘dangerous Event II’ until the $T_{p2} > \text{safety threshold}$ or the driver’s attention return to the road.
Yes	$N \times T_{hrzn} + T_{p2} \leq \text{or} > \text{safety threshold}$	Provide warning: Look back to the road immediately.

detection system is installed) the system should warn the driver to look back to the road without getting distracted for a long time. A shorter  $T_{p2} + N \times T_{hrzn}$  than the safety threshold indicates a relatively safe map-glance action. In that case, when there is no hazard detected (or no detection system is installed), the system continues to monitor EEG signals and keeps on predicting the “dangerous Event II” until  $T_{p2} + N \times T_{hrzn}$  is longer than the safety threshold or the driver returns to the road.

However, when there is a hazard event being detected, a delay to return to the road may lead to less time to respond to the hazard and cause dangerous situations. Therefore, the system should alert the driver to watch out for the hazard immediately, whether  $T_{p2} + N \times T_{hrzn}$  is longer or shorter than the safety threshold.

### C. Practical Applications of EEG Techniques

From a practical application standpoint, the EEG technique applied in this study has its advantages in several situations compared to eye movement tracking used in previous studies. First, it enables the system to obtain a driver’s cognitive activities in real time and provide appropriate feedbacks to assist the driver. The performance of the eye-movement-tracking-based methods can be seriously deteriorated in the presence of strong light, while EEG signals are usually stable under various environmental conditions. This characteristic of EEG data is really attractive in the real-world applications. In addition, EEG data are superior to protect driver privacy without recording any personal information. With even higher privacy standard in the current market, drivers would accept a system with techniques of high-standard privacy protection more easily.

Although this study was carefully prepared, there are still several limitations. First of all, although the proposed computational prediction approach provides a promising tool to improve the current design of driving assistant systems, the influence of the driver-distraction prediction on driving behaviors is unknown. For example, the false predictions may also incur extra distractions and annoyance to drivers. This problem will be addressed in the future work. Second, the reaction period that allows drivers to respond to the prediction outcomes was not considered in the current work. Reaction time can be used to evaluate whether a driver has enough time to react to an upcoming event or note. To enhance the practical utility of the proposed ATP prediction framework in the design of new navigation systems, we will consider the reaction time in the

prediction system in future work. In addition, we employed the conventional wired wet EEG electrodes in the present experimental setup, which are difficult and inconvenient to be applied for real-world applications. In the further work, we will test EEG devices with dry electrodes and wireless data transfer function, and investigate the prediction power and stabilization of the remotely collected EEG data from dry electrodes.

## VI. CONCLUSION

In this paper, we have investigated the online monitoring and prediction of driver distraction using EEG signals of 24 subjects. We propose an adaptive online prediction framework that is capable of capturing subject-specific predictive patterns autonomously by constructing a subject-specific pattern library, based on which a probabilistic prediction rule is established. The proposed online prediction system achieved promising prediction results with overall prediction accuracy of 81% for Event I and 70% for Event II. Under the best performance settings, the average prediction time of Event I is 234 ms ahead of the real occurrence of Event I, and the average prediction of Event II is 430 ms ahead of the real occurrence of Event II. The proposed methodology provides a practical tool to solve the challenging problem of online predicting of driver distraction using multivariate EEG signals. It has a potential to improve design of future intelligent navigation systems from a novel perspective, by preventing driver distractions in advance and the related safety risks.

## ACKNOWLEDGMENT

We really appreciate the support from NSF for this work and we also appreciate the valuable suggestions from the anonymous reviewers in improving this work.

## REFERENCES

- [1] U.S. Department of Transportation, National Highway Traffic Safety Administration. (2012). Distracted Driving 2010, NHTSA'S Nat. Center Stat. Anal., Washington, DC, USA, DOT HS 811 650. [Online]. Available: <http://www-nrd.nhtsa.dot.gov/Pubs/811650.pdf>
- [2] T. Ranney, "Driver distraction: A review of the current state-of-knowledge," Nat. Highway Traffic Safety Admin. Veh. Res. Test Center, Washington D.C, Tech. Rep. DOT HS 810 787, Apr. 2008.
- [3] B. Donmez, L. N. Boyle, and J. D. Lee, "Differences in off-road glances: Effects on young drivers' performance," *J. Transp. Eng.*, vol. 136, no. 5, pp. 403–409, May 2010.
- [4] B. Donmez, L. N. Boyle, and J. D. Lee, "Safety implications of providing real-time feedback to distracted drivers," *Accident Anal. Prev.*, vol. 39, no. 3, pp. 581–590, May 2007.
- [5] Y. Liang and J. D. Lee, "Combining cognitive and visual distraction: Less than the sum of its parts," *Accident Anal. Prev.*, vol. 42, no. 3, pp. 881–890, May 2010.
- [6] W. J. Horrey and C. D. Wickens, "Examining the impact of cell phone conversations on driving using meta-analytic techniques," *Hum. Factors*, vol. 48, no. 1, pp. 196–205, Mar. 2006.
- [7] S. L. Chisholm, J. K. Caird, and J. Lockhart, "The effects of practice with MP3 players on driving performance," *Accident Anal. Prev.*, vol. 40, no. 2, pp. 704–713, Mar. 2008.
- [8] H.-H. Chiang, J.-W. Perng, B.-F. Wu, S.-J. Wu, and T.-T. Lee, "The human-in-the-loop design approach to the longitudinal automation system for the intelligent vehicle, TAIWAN ITS-i," in *Proc. IEEE Int. Conf. Syst., Man Cybern.*, Oct. 2006, pp. 383–388.
- [9] M. L. Reyes and J. D. Lee, "Effects of cognitive load presence and duration on driver eye movements and event detection performance," *Transp. Res. F, Traffic Psychol. Behav.*, vol. 11, no. 6, pp. 391–402, Nov. 2008.
- [10] J. D. Lee and D. L. Strayer, "Preface to the special section on driver distraction," *Hum. Factors*, vol. 46, no. 4, pp. 583–586, Jan. 2004.
- [11] Y. C. Liu, "Comparative study of the effects of auditory, visual and multimodality displays on drivers' performance in advanced traveller information systems," *Ergonomics*, vol. 44, no. 4, pp. 425–442, Mar. 2001.
- [12] G. Vashitz, D. Shinar, and Y. Blum, "In-vehicle information systems to improve traffic safety in road tunnels," *Transp. Res. F, Traffic Psychol. Behav.*, vol. 11, no. 1, pp. 61–74, Jan. 2008.
- [13] C. L. Baldwin, "Verbal collision avoidance messages during simulated driving: Perceived urgency, alerting effectiveness and annoyance," *Ergonomics*, vol. 54, no. 4, pp. 328–337, Apr. 2011.
- [14] J. Fagerlönn, "Urgent alarms in trucks?: Effects on annoyance and subsequent driving performance," *IET Intell. Transp. Syst.*, vol. 5, no. 4, pp. 1–24, Dec. 2011.
- [15] C.-T. Lin *et al.*, "EEG-based assessment of driver cognitive responses in a dynamic virtual-reality driving environment," *IEEE Trans. Biomed. Eng.*, vol. 54, no. 7, pp. 1349–1352, Jul. 2007.
- [16] C.-T. Lin, S.-A. Chen, T.-T. Chiu, H.-Z. Lin, and L.-W. Ko, "Spatial and temporal EEG dynamics of dual-task driving performance," *J. Neuroeng. Rehabil.*, vol. 8, no. 1, p. 11, Feb. 2011.
- [17] M. M. Spapé and D. J. Serrien, "Prediction of collision events: An EEG coherence analysis," *Clin. Neurophysiol.*, vol. 122, no. 5, pp. 891–896, May 2011.
- [18] B. Metz, N. Schömig, and H.-P. Krüger, "Attention during visual secondary tasks in driving: Adaptation to the demands of the driving task," *Transp. Res. F, Traffic Psychol. Behav.*, vol. 14, no. 5, pp. 369–380, Sep. 2011.
- [19] H. Zhang, M. R. H. Smith, and G. J. Witt, "Identification of real-time diagnostic measures of visual distraction with an automatic eye-tracking system," *Hum. Factors*, vol. 48, no. 4, pp. 805–821, Dec. 2006.
- [20] D. W. Hansen and A. E. C. Pece, "Eye tracking in the wild," *Comput. Vis. Image Understand.*, vol. 98, no. 1, pp. 155–181, Apr. 2005.
- [21] J. Chiou, L. Ko, and C. Lin, "Using novel MEMS EEG sensors in detecting drowsiness application," in *Proc. IEEE Biomed. Circuits Syst. Conf.*, 2006, no. 95, pp. 33–36.
- [22] C.-T. Lin *et al.*, "Novel dry polymer foam electrodes for long-term EEG measurement," *IEEE Trans. Biomed. Eng.*, vol. 58, no. 5, pp. 1200–1207, May 2011.
- [23] T. J. Sullivan, S. R. Deiss, and G. Cauwenberghs, "A low-noise, non-contact EEG/ECG sensor," in *Proc. IEEE Biomed. Circuits Syst. Conf.*, 2007, pp. 154–157.
- [24] B. Donmez, L. N. Boyle, and J. D. Lee, "Mitigating driver distraction with retrospective and concurrent feedback," *Accident Anal. Prev.*, vol. 40, no. 2, pp. 776–786, Mar. 2008.
- [25] L. Garay-Vega *et al.*, "Evaluation of different speech and touch interfaces to in-vehicle music retrieval systems," *Accident Anal. Prev.*, vol. 42, no. 3, pp. 913–920, May 2010.
- [26] D. B. Kaber, Y. Liang, Y. Zhang, M. L. Rogers, and S. Gangakhedkar, "Driver performance effects of simultaneous visual and cognitive distraction and adaptation behavior," *Transp. Res. F, Traffic Psychol. Behav.*, vol. 15, no. 5, pp. 491–501, Sep. 2012.
- [27] K. L. Young, E. Mitsopoulos-Rubens, C. M. Rudin-Brown, and M. G. Lenné, "The effects of using a portable music player on simulated driving performance and task-sharing strategies," *Appl. Ergonom.*, vol. 43, no. 4, pp. 738–746, Jul. 2012.
- [28] Y. Zhang *et al.*, "Driver distraction and performance effects of highway logo sign design," *Appl. Ergonom.*, vol. 44, no. 3, pp. 472–479, May 2013.
- [29] J. Stutts *et al.*, "Driver's exposure to distractions in their natural driving environment," *Accident Anal. Prev.*, vol. 37, no. 6, pp. 1093–1101, Nov. 2005.
- [30] C. Wege, S. Will, and T. Victor, "Eye movement and brake reactions to real world brake-capacity forward collision warnings—A naturalistic driving study," *Accident Anal. Prev.*, vol. 58, pp. 259–270, Sep. 2013.
- [31] H. Alm and L. Nilsson, "The effects of a mobile telephone task on driver behaviour in a car following situation," *Accident Anal. Prev.*, vol. 27, no. 5, pp. 707–715, Oct. 1995.
- [32] J. Greenberg, L. Tijerina, and R. Curry, "Driver distraction: Evaluation with event detection paradigm," *Transp. Res. Rec., J. Transp. Res. Board*, vol. 1843, no. 1, pp. 1–9, 2003.
- [33] K. L. Young and P. M. Salmon, "Examining the relationship between driver distraction and driving errors: A discussion of theory, studies and methods," *Safety Sci.*, vol. 50, no. 2, pp. 165–174, Feb. 2012.
- [34] M. Reed and P. Green, "Comparison of driving performance on-road and in a low-cost simulator using a concurrent telephone dialling task," *Ergonomics*, vol. 42, no. 8, pp. 1015–1037, Aug. 1999.

- [35] K. L. Young, M. G. Lenné, and A. R. Williamson, "Sensitivity of the lane change test as a measure of in-vehicle system demand," *Appl. Ergonom.*, vol. 42, no. 4, pp. 611–618, May 2011.
- [36] M. Mouloua, A. Ahern, and A. Quevedo, "The effects of iPod and text-messaging use on driver distraction: A bio-behavioral analysis," *Work*, vol. 41, no. 1, pp. 5886–5888, 2012.
- [37] A. Sonnleitner, M. Simon, W. E. Kincses, A. Buchner, and M. Schrauf, "Alpha spindles as neurophysiological correlates indicating attentional shift in a simulated driving task," *Int. J. Psychophysiol.*, vol. 83, no. 1, pp. 110–118, Jan. 2012.
- [38] C. Lin, L. Ko, and T. Shen, "Computational intelligent brain computer interaction and its applications on driving cognition," *IEEE Comput. Intell. Mag.*, vol. 4, no. 4, pp. 32–46, Nov. 2009.
- [39] K. Young, M. Regan, and M. Hammer, "Driver distraction: A review of the literature," in *Distacted Driving*. Sydney, N.S.W., Australia: Australasian College of Road Safety, 2007, pp. 379–405.
- [40] M. Sodhi, B. Reimer, and I. Llamazares, "Glance analysis of driver eye movements to evaluate distraction," *Behav. Res. Methods, Instrum., Comput.*, vol. 34, no. 4, pp. 529–538, Nov. 2002.
- [41] S. Klauer, T. Dingus, and V. Neale, "The impact of driver inattention on near-crash/crash risk: An analysis using the 100-car naturalistic driving study data," Nat. Highway Traffic Safety Admin., Washington, DC, USA, Tech. Rep. DOT HS 810 594, Aug. 2006.
- [42] P. Pudil, J. Novovičová, and J. Kittler, "Floating search methods in feature selection," *Pattern Recognit. Lett.*, vol. 15, no. 11, pp. 1119–1125, Nov. 1994.
- [43] F. Mormann, R. G. Andrzejak, C. E. Elger, and K. Lehnertz, "Seizure prediction: The long and winding road," *Brain, J. Neurol.*, vol. 130, no. 2, pp. 314–333, Feb. 2007.
- [44] S. Haufe *et al.*, "EEG potentials predict upcoming emergency brakings during simulated driving," *J. Neural Eng.*, vol. 8, no. 5, p. 056001, Oct. 2011.
- [45] C. Berka *et al.*, "EEG correlates of task engagement and mental workload in vigilance, learning, memory tasks," *Aviat., Space, Environ. Med.*, vol. 78, no. S, pp. B231–B244, May 2007.
- [46] F. Elliott and C. Louttit, "Auto braking reaction times to visual vs. auditory warning signals," *Proc. Indiana Acad. Sci.*, vol. 47, no. 1937, pp. 220–225, 2013.
- [47] R. Kosinski, A literature review on reaction time, Clemson Univ., Clemson, SC, USA, Tech. Rep. [Online]. Available: <http://biae.clemson.edu/bpc/bp/Lab/110/reaction.htm>
- [48] S. M. Zhou, J. Q. Gan, and F. Sepulveda, "Classifying mental tasks based on features of higher-order statistics from EEG signals in brain-computer interface," *Inf. Sci.*, vol. 178, no. 6, pp. 1629–1640, Mar. 2008.
- [49] S. M. S. Alam and M. I. H. Bhuiyan, "Detection of seizure and epilepsy using higher order statistics in the EMD domain," *IEEE J. Biomed. Health Informat.*, vol. 17, no. 2, pp. 312–318, Mar. 2013.
- [50] R. Esteller, J. Echauz, and T. Tchong, "Comparison of line length feature before and after brain electrical stimulation in epileptic patients," in *Proc. 26th Int. Conf. IEEE Eng. Med. Biol. Soc.*, 2004, pp. 4710–4713.
- [51] S. Wang, C. J. Lin, C. Wu, and W. Chaovaitwongse, "Early detection of numerical typing errors using data mining techniques," *IEEE Trans. Syst., Man, Cybern. A, Syst., Humans*, vol. 41, no. 6, pp. 1199–1212, Nov. 2011.
- [52] S. Wong, G. H. Baltuch, J. L. Jaggi, and S. F. Danish, "Functional localization and visualization of the subthalamic nucleus from microelectrode recordings acquired during DBS surgery with unsupervised machine learning," *J. Neural Eng.*, vol. 6, no. 2, p. 026006, Apr. 2009.
- [53] R. Agarwal and J. Gotman, "Adaptive segmentation of electroencephalographic data using a nonlinear energy operator," in *Proc. IEEE Int. Symp. Circuits Syst.*, 1999, vol. 4, pp. 199–202.
- [54] S. Sun, "The extreme energy ratio criterion for EEG feature extraction," in *Artificial Neural Networks*, vol. 5164. Berlin, Germany: Springer-Verlag, 2008, ser. Lecture Notes in Computer Science, pp. 919–928.
- [55] S. Sun, "Extreme energy difference for feature extraction of EEG signals," *Expert Syst. Appl.*, vol. 37, no. 6, pp. 4350–4357, Jun. 2010.
- [56] W. Chaovaitwongse, R. S. Pottenger, S. Wang, Y.-J. Fan, and L. D. Iasemidis, "Pattern-and network-based classification techniques for multichannel medical data signals to improve brain diagnosis," *IEEE Trans. Syst., Man, Cybern. A, Syst., Humans*, vol. 41, no. 5, pp. 977–988, Sep. 2011.
- [57] S. Sun and C. Zhang, "Adaptive feature extraction for EEG signal classification," *Med. Biol. Eng. Comput.*, vol. 44, no. 10, pp. 931–935, Oct. 2006.
- [58] O. A. Rosso *et al.*, "Wavelet entropy: A new tool for analysis of short duration brain electrical signals," *J. Neurosci. Methods*, vol. 105, no. 1, pp. 65–75, Jan. 2001.



**Shouyi Wang** received the B.S. degree in control science and engineering from Harbin Institute of Technology, Harbin, China, in 2003; the M.S. degree in systems and control engineering from Delft University of Technology, Delft, The Netherlands, in 2005; and the Ph.D. degree in industrial and systems engineering from Rutgers University, Piscataway, NJ, USA, in 2012.

From 2012 to 2013, he was a Research Associate with the Department of Industrial and Systems Engineering and the Integrated Brain Imaging Center, University of Washington, Seattle, WA, USA. He is currently an Assistant Professor of industrial and manufacturing systems engineering with University of Texas at Arlington, Arlington, TX, USA. His research interests include data mining and pattern discovery, machine learning, intelligent decision-making systems, and multivariate time-series modeling and forecasting.



**Yiqi Zhang** received the B.S. degree in psychology from Zhejiang University, Hangzhou, China, in 2011. She is currently working toward the Ph.D. degree with the Department of Industrial and System Engineering, The State University of New York, Buffalo, NY, USA.

Her research interest includes the development of mathematical models of human response in the interaction with engineering systems and addressing human cognition with their application in the design of the intelligent transportation systems.



**Changxu Wu** (S'04–M'07) received the M.S. and Ph.D. degrees in industrial and operational engineering from University of Michigan, Ann Arbor, MI, USA, in 2004 and 2007, respectively.

Currently he is an Associate Professor with the Department of Industrial and System Engineering, The State University of New York, Buffalo, NY, USA, where he directs the Cognitive System Laboratory. He is interested in integrating cognitive science and engineering system design, particularly modeling the human cognition system with its applications in system design, improving transportation safety, promoting human performance in human–computer interaction, and inventing innovative sustainable and smart energy systems with human in the loop. He has published more than 36 journal papers in various fields.

He is Associate Editor for *IEEE TRANSACTIONS ON INTELLIGENT TRANSPORTATION SYSTEMS* and *Behavior and Information Technology Journal*.



**Felix Darvas** received the B.S., M.S., and Ph.D. degrees from the Rheinische-Westfaelische Technische Hochschule (RWTH), Aachen, Germany, in 1993, 1998, and 2002, respectively, all in physics.

From 2002 to 2006 he was a Postdoctoral Research Fellow and Research Faculty with University of Southern California, Los Angeles, CA, USA, where he was working on imaging techniques and statistical analysis for magnetoencephalographic/electroencephalographic and molecular imaging. He is currently a Research Assistant Professor with the

Department of Neurosurgery, University of Washington, Seattle, WA, USA, where his research interests include brain machine interfaces, functional cortical networks, and the human motor system.



**Wanpracha Art Chaovaitwongse** (SM'11) received the Ph.D. degree in industrial and systems engineering from University of Florida, Gainesville, FL, USA.

He is an Associate Professor of industrial and systems engineering and radiology (joint) with University of Washington, Seattle, WA, USA, where he is a core member of the Integrated Brain Imaging Center. His research interests include optimization and machine learning in neurophysiological and imaging data.